Simulation of Structure Formation in an Electrorheological Fluid

R. Tao and Qi Jiang
Department of Physics, Southern Illinois University, Carbondale, Illinois 62901
(Received 21 October 1993)

The temporal evolution of three-dimensional structure in an electroheological (ER) fluid is examined by a computer simulation. A parameter B characterizing the ratio of the Brownian force to the dipolar force is introduced. For a wide range of B, the ER fluid has a rapid chain formation followed by aggregation of chains into thick columns which has a body-centered tetragonal lattice structure. The Peierls-Landau instability of single chains helps formation of thick columns. If the Brownian force is very small, the ER system may be trapped in some local energy-minimum state.

PACS numbers: 82.70.Gg, 61.90.+d, 64.90.+b

Electrorheological (ER) fluids, often referred to as smart fluids, have a wide variety of applications in industries and technologies. A typical ER fluid consists of a suspension of fine dielectric particles in a liquid of low dielectric constant [1]. Its effective viscosity increases dramatically if an electric field is applied, and when the field exceeds a critical value, the ER fluid turns into a solid. These phenomena occur in milliseconds and are reversible.

The structure is fundamental in understanding the physical mechanism and properties of ER fluids. Experiments find that upon application of electric field, dielectric particles in ER fluids rapidly form chains which then aggregate into thick columns [2–5]. A theoretical prediction [6] of a body-centered tetragonal (bct) lattice as the ground state of the thick columns has recently been verified by experiments [2]. The issue of dynamics of structure formation in ER fluids is under extensive investigation. Since Kamien and Nelson recently pointed out that phase transition in ER fluids is related to the physics of directed polymer and quantum mechanics of bosons in $2+1$ dimensions [7,8], the interest in the issue has further been enhanced.

Two-dimensional (2D) computer simulations were first employed to investigate the issue. If thermal fluctuations are ignored, 2D simulations find separated single chains when the short-range repulsive force is $\sim 1/r^{13}$ or mostly double-width strands if the repulsive force is exponential [9]. Computer simulations on the same model of exponential repulsion with thermal fluctuations found many thick columns of close-packed triangular lattice [10]. Extrapolation of the 2D results to three-dimensional (3D) systems, however, is hindered.

There have been a couple of 3D simulations of ER fluids reported. Whittle [11] and Heyes and Melrose [12] only examined the initial aggregation process in their 3D simulations peripherally. The simulations by Bonnecaze and Brady [13] include the full hydrodynamics and electrostatics, but are performed at zero temperature, thus do not give information on the structure formed. Recently, Hass reported that a regular lattice was not formed in his 3D simulation [14]. However, his simulation ignores the thermal fluctuations which are important in formation of thick columns [5].

To clarify the issue, we consider a monodisperse suspension of spherical dielectric particles in a nonconducting liquid. The particles have diameter σ and dielectric constant ϵ_p. The liquid has dielectric constant ϵ_f and viscosity η. The system is confined between two parallel electrodes, planes $z=0$ and $z=L$. When there is no voltage applied, the particles are randomly distributed throughout the fluid. In an electric field, each particle obtains an induced dipole moment, $\mathbf{p}=\alpha\epsilon_f(\sigma/2)^3\mathbf{E}_{\rm loc}$ where $\alpha=(\epsilon_p-\epsilon_f)/(\epsilon_p+2\epsilon_f)$ and $\mathbf{E}_{\rm loc}$ is the local field. The motion of the ith particle is described by a Langevin equation

$$m d^2\mathbf{r}_i/dt^2=\mathbf{F}_i-3\pi\sigma\eta d\mathbf{r}_i/dt+\mathbf{R}_i(t)\,, \tag{1}$$

where $\mathbf{F}_i$ is the electric force and $-3\pi\sigma\eta\mathbf{v}_i$ is the Stokes' drag force, the leading hydrodynamic force on the particle. As was done in other simulations [9–12,14], we take the dipolar approximation. The role of higher order multipoles will be discussed later. A random Brownian force $\mathbf{R}_i(t)$ in Eq. (1) represents the net effect of collisions of solvent molecules on the particle.

We have found that the thermal motion plays a very important role in the structure formation of ER fluids. Though for a typical ER fluid the dipolar energy is much stronger than the thermal energy, $(p^2/\epsilon_f\sigma^3)/k_BT\sim 10^6$, the thermal energy cannot be ignored. Because of the Peierls-Landau instability of one-dimensional solid, a ratio of the thermal energy to the lowest phonon excitation energy of a single chain is much bigger than unity [5]. The thermal energy is more than sufficient in creating thermal vibrations of the single chains which help the aggregation process. We will introduce a parameter, B, characterizing the ratio of the dipolar force to the Brownian force. Our simulation finds that for a wide range of B, with the help of the Brownian force, the ER fluid evolves into thick columns which have the bct lattice structure.

The dipolar force acting on the particle at $\mathbf{r}_i$ by a particle at $\mathbf{r}_j$ is given by

$$\mathbf{f}_{ij}=(3p^2/\epsilon_f r_{ij}^4)[\mathbf{e}_r(1-3\cos^2\theta_{ij})-\mathbf{e}_\theta\sin(2\theta_{ij})]\,, \tag{2}$$

where $\mathbf{r}_{ij}=\mathbf{r}_i-\mathbf{r}_j$ and $0\le\theta_{ij}\le\pi/2$ is the angle between

0031-9007/94/73(1)/205(4)$06.00

the z direction and the joint line of the two dipoles. We use $\mathbf{e}_r$ as a unit vector parallel to $\mathbf{r}_{ij}$ and $\mathbf{e}_\theta$ as a unit vector parallel to $\mathbf{e}_r \times (\mathbf{e}_r \times \mathbf{E}_0)$. A dipole $\mathbf{p}$ inside the capacitor at $\mathbf{r}_i = (x_i, y_i, z_i)$ produces an infinite number of images at $(x_i, y_i, -z_i)$ and $(x_i, y_i, 2Lk \pm z_i)$ for $k = \pm 1, \pm 2, \ldots$. The force between a dipole and an image has the same form as Eq. (2). The jth particle and its infinite images produce an electric force on the ith particle,

$$f_{ij,x} = \frac{p^2}{\epsilon_f L^4} \sum_{s=1}^{\infty} \frac{4s^3\pi^3(x_i - x_j)}{\rho_{ij}} K_1\left(\frac{s\pi\rho_{ij}}{L}\right) \cos\left(\frac{s\pi z_i}{L}\right) \cos\left(\frac{s\pi z_j}{L}\right),$$

$$f_{ij,y} = \frac{p^2}{\epsilon_f L^4} \sum_{s=1}^{\infty} \frac{4s^3\pi^3(y_i - y_j)}{\rho_{ij}} K_1\left(\frac{s\pi\rho_{ij}}{L}\right) \cos\left(\frac{s\pi z_i}{L}\right) \cos\left(\frac{s\pi z_j}{L}\right), \tag{3}$$

$$f_{ij,z} = \frac{p^2}{\epsilon_f L^4} \sum_{s=1}^{\infty} 4s^3\pi^3 K_0\left(\frac{s\pi\rho_{ij}}{L}\right) \sin\left(\frac{s\pi z_i}{L}\right) \cos\left(\frac{s\pi z_j}{L}\right),$$

where $\rho_{ij} = \sqrt{(x_i - x_j)^2 + (y_i - y_j)^2}$ and K_0 and K_1 are modified Bessel functions. The force on the ith particle by its own images is in the z direction and denoted as $\mathbf{f}_i^{\text{self}}$,

$$f_{i,z}^{\text{self}} = \frac{3p^2}{8\epsilon_f}\left[-\frac{1}{z_i^4} + \sum_{s=1}^{\infty}\left[\frac{1}{(z_i - sL)^4} - \frac{1}{(z_i + sL)^4}\right]\right]. \tag{4}$$

To simulate the hard spheres and hard walls, we introduce a short-range repulsive force between two particles

$$\mathbf{f}_{ij}^{\text{rep}} = (3p^2\mathbf{e}_r/\epsilon_f\sigma^4)\exp[-100(r_{ij}/\sigma - 1)] \tag{5}$$

and a short-range repulsion between a particle and the electrodes

$$\mathbf{f}_i^{\text{wall}} = (3p^2\mathbf{e}_z/\epsilon_f L^4)\{\exp[-100(z_i/\sigma - 0.5)] - \exp[-100((L - z_i)/\sigma - 0.5)]\}. \tag{6}$$

Now $\mathbf{F}_i$ in Eq. (1) is given by $\mathbf{F}_i = \sum_{j\neq i}(\mathbf{f}_{ij} + \mathbf{f}_{ij}^{\text{rep}}) + \mathbf{f}_i^{\text{self}} + \mathbf{f}_i^{\text{wall}}$. The random force $\mathbf{R}_i(t)$ has a white-noise distribution, $\langle R_{i,\alpha}(0) R_{i,\beta}(t)\rangle = 6\pi k_B T\sigma\eta\delta_{\alpha\beta}\delta(t)$ and $\langle R_{i,\alpha}\rangle = 0$ where k_B is Boltzmann's constant and T is the temperature. We introduce a subinterval τ which is well defined in the Brownian motion [15]. This time τ is longer than the molecular collision time, but quite small on macroscopic scale, therefore, shorter than the time steps used in integration of Eq. (1). During τ we can treat all functions of time except $\mathbf{R}(t)$ as constants. Then, the average of $\mathbf{R}_i(t)$ over τ, $R_{i,\alpha}(t,\tau) = (1/\tau) \times \int_t^{t+\tau} R_{i,\alpha}(t')dt'$, has a Gaussian distribution

$$W(R_{i,\alpha}(t,\tau)) = \frac{1}{(2\pi)^{1/2}\Omega}\exp\{-[R_{i,\alpha}(t,\tau)]^2/2\Omega^2\}, \tag{7}$$

where $\Omega = \sqrt{6\pi k_B T\sigma\eta/\tau}$. For any $X_\alpha = \int_t^{t+\delta t}\psi(\xi) \times R_{i,\alpha}(\xi)d\xi$ with a smooth function ψ on a time step $\delta t > \tau$, we can divide δt into many subintervals of duration τ. X_α has a probability distribution

$$W(X_\alpha) = (\pi q)^{-1/2}\exp(-X_\alpha^2/q), \tag{8}$$

where $q = 2\Omega^2\tau\int_t^{t+\delta t}\psi^2(\xi)d\xi$ is independent of τ. This implies that our result is independent of a specific choice of τ, though the value of τ is not very uniquely defined.

The intrinsic time scale in Eq. (1) is $t_0 = m/3\pi\sigma\eta$. We take $t = t_0 t^*$, $\mathbf{F}_i = F_0\mathbf{F}_i^*$ where $F_0 = 3p^2/\epsilon_f\sigma^4$, $\mathbf{R}_i = \Omega\mathbf{R}_i^*(t)$, and $\mathbf{r}_i = \sigma\mathbf{r}_i^*$ in Eq. (1). The scaling transformation produces a new equation,

$$\ddot{\mathbf{r}}_i^* + \dot{\mathbf{r}}_i^* = A(\mathbf{F}_i^* + B\mathbf{R}_i^*), \tag{9}$$

where $A = F_0/3\pi\sigma\eta(\sigma/t_0)$ and $B = \Omega/F_0$. It is clear that $1/A$ is related to the Mason number, a ratio of the viscous force to the dipolar force. B is a ratio of the Brownian force to the dipolar force and $1/AB^2$ is related to parameter $\lambda = (p^2/\epsilon_f\sigma^3)/k_B T$ [16]. Since the Brownian force depends on both temperature T and viscosity η, B is a better parameter in discussion of the Brownian motion than λ which is independent of η.

Equation (9) indicates that the final structure of our system is related to the two constants A and B. For an ER system of alumina particles in petroleum oil, $\epsilon_f \sim 2$, $\epsilon_p \sim 8$, $\eta \sim 0.2$ P, $\sigma \sim 10$ μm, and the mass density of the particle $\rho \sim 3$ g/cm^3. At $E_0 = 3$ kV/mm and $T = 300$ K, the ER fluid will be solidified in experiments. We estimate $t_0 \sim 8.33\times10^{-7}$ s and $A \sim 10^{-4}$ under these conditions and choose $\tau = 0.4t_0$ to meet the aforesaid condition. Then, $B \sim 10^{-1}$. Our simulation takes A and B around the above values.

We have applied two Runge-Kutta methods to integrate Eq. (9): (1) of a fixed step size and (2) of adaptive step-size control. Though both give the same results, the method of adaptive step-size control is much more efficient, in which the time step δt varies according to moves of particles [17]. We specify a criterion δr_c. If the largest position change among all particles after δt is smaller than δr_c, the time step δt in the subsequent integration will be increased. Otherwise, δt will be reduced. In both methods, Eq. (8) must be employed to treat the Brownian force [15]. As mentioned before, the integration of Eq. (9) is independent on τ.

Our simulation has $N = 122$ particles in a box with $L_x = L_y = 5\sigma$ and $L_z = 14\sigma$ which has a volume fraction

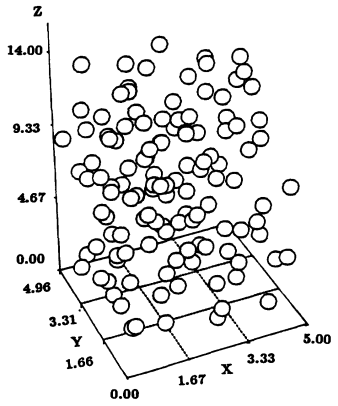

FIG. 1. In the initial state, dielectric particles are randomly distributed.

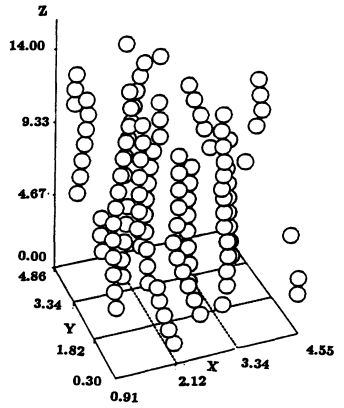

FIG. 3. The configuration after 20000 time steps.

$\phi=0.183$. Theoretical calculation has already shown that if $L_z \leq 6\sigma$, the single-chain structure has a lower energy than that of thick columns [6]. Therefore, we take a relatively big L_z. A periodic boundary condition is imposed in the x and y directions. At every step, we apply the following three order parameters to characterize the structure [18],

$$\rho_j = \left| \frac{1}{N} \sum_{i=1}^{N} \exp(i\mathbf{b}_j \cdot \mathbf{r}_i) \right|, \tag{10}$$

where three reciprocal lattice vectors of the bct lattice $\mathbf{b}_1=(2\pi/\sigma)(2\mathbf{e}_x'/\sqrt{6}-\mathbf{e}_z)$, $\mathbf{b}_2=(2\pi/\sigma)(2\mathbf{e}_y'/\sqrt{6}-\mathbf{e}_z)$, and $\mathbf{b}_3=4\pi\mathbf{e}_z/\sigma$. The unit vector $\mathbf{e}_z$ is (001) lattice axis along the field direction, but $\mathbf{e}_x'$ and $\mathbf{e}_y'$ are the bct lattice axes (100) and (010). In the structure formation, the ER system may rotate around the z axis. Therefore, when measuring ρ_1 and ρ_2, we always rotate $\mathbf{e}_x'$ and $\mathbf{e}_y'$ about the z axis to find a position which maximizes $\rho_1\rho_2$. The order parameter ρ_3 characterizes the formation of chains in the z direction. The other two parameters ρ_1 and ρ_2 characterize the structure in the x-y plane.

The initial state is shown in Fig. 1 where the dielectric particles are randomly distributed and the three order parameters are vanishing. At $t=0$, a strong electric field is turned on and the particles begin to move. It can be noticed from Fig. 2 that after the first 5000 steps (about 10 ms), single chains are in shape but the lateral ordering is very weak. The structure has $\rho_3=0.617$, while $\rho_1=0.32$ and $\rho_2=0.16$. At the end of the next 15000 steps, we have $\rho_3=0.92$, but ρ_1 and ρ_2 remain around 0.4–0.5 (Fig. 3). Clearly, the ordering in the field direction is almost perfect and the lateral ordering is building. The structure after 90000 steps (Fig. 4) clearly shows excellent orderings both in the field direction and in the x-y plane. Single chains have been aggregated into a bct lattice structure. Three order parameters are $\rho_3=0.991$, $\rho_1=0.915$, and $\rho_2=0.850$. Further time evolution shows little improvement and the process becomes extremely slow.

The projection of the 3D structure in Fig. 4 onto the x-y plane has a square lattice on the x-y plane (Fig. 5). For example, the marked square has its side $\simeq\sqrt{1.5}\sigma=1.225\sigma$, marking an ideal bct lattice. The four chains at the corners have 14 particles straight along the field direction. The chain at the center has 12 particles close packed with the four neighbor chains. The structure is an ideal bct lattice if the chain at the center does not have one particle missing. The thick dots in Fig. 5 also indi-

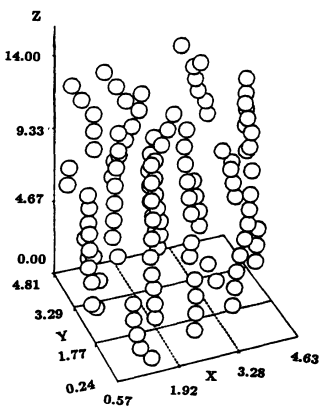

FIG. 2. The configuration after first 5000 time steps.

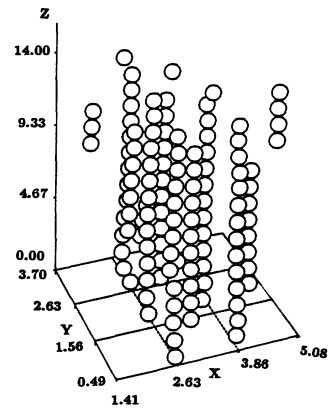

FIG. 4. The configuration after 90000 time steps.

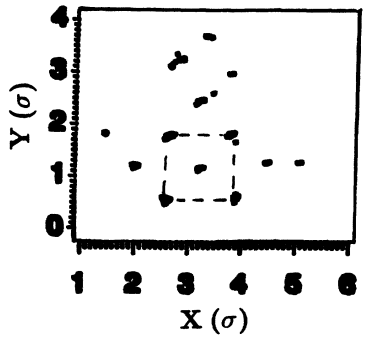

FIG. 5. Projection of the configuration in Fig. 4 to the x-y plane.

cate that the chains are straight in the field direction.

Figure 6 shows the development of ρ_i $(i=1,2,3)$ with time. The formation of single chains is rapid. In about several milliseconds, ρ_3 reaches 0.6. After 0.4 s, ρ_3 is above 0.9. The building of lateral ordering is relatively slower than the formation of chain. It takes about several seconds to have ρ_1 and ρ_2 reach 0.8. The strong fluctuations of ρ_1 and ρ_2 after the formation of chains are consistent with experiments [3], signifying the aggregation of separated chains into columns.

We have also done some tests to verify the importance of Brownian force in the development of ER solid structure. If we ignore the Brownian motion completely, or let B be extremely small, such as $B\sim 10^{-6}$, the ER fluid has a rapid chain formation followed by a kinetic trapping into a complicated structure [14]. After a long time, the structure has ρ_3 remaining at about 0.7 but ρ_1 and ρ_2 remain 0.3 or below. The structure in such a case needs further study because it may be related to directed polymers [7]. When $B\gg 1$, the ER system has too many vibrations, preventing the formation of a stable structure. However, for quite a wide range of B, the ER fluid has a rapid chain formation, followed by an aggregation of chains into the bct lattice structure with three order parameters close to or above 0.9. We have also found the bct lattice when volume fraction $\phi \geq 20\%$. If ϕ further

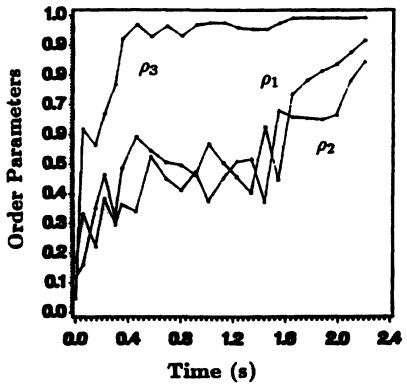

FIG. 6. The order parameters change with time after the electric field is applied. The time unit is seconds.

increases, the system may be easy to develop into thick columns of a polycrystalline structure which have several bct lattice grains with the same (001) axis but different (100) and (010) axes [2]. Finally, we compare the time scales in our simulation with that in the experiments. The rapid chain formation takes about 10 ms or longer in our simulation. This result, consistent with other simulations [9], is longer than the experimental result [19]. The reason for this difference may lie in the fact that we ignore the contributions from higher multipoles, charges, and currents in ER fluids which begin to draw attention recently [20].

This research is supported by the Office of Naval Research Grant No. N00014-93-1-0582.

[1] For example, see *Electrorheological Fluids*, edited by R. Tao (World Scientific, Singapore, 1992); H. Block and J. P. Kelly, U.S. Patent No. 4687589 (1987); F. E. Filisko and W. E. Armstrong, U.S. Patent No. 4744914 (1988).

[2] T. J. Chen, R. N. Zitter, and R. Tao, Phys. Rev. Lett. **68**, 2555 (1992).

[3] J. E. Martin, J. Odinek, and T. C. Halsey, Phys. Rev. Lett. **69**, 1524 (1992).

[4] J. M. Ginder and L. D. Elie, *Electrorheological Fluids*, in (Ref. [1]), p. 23.

[5] T. C. Halsey and W. Toor, Phys. Rev. Lett. **65**, 2820 (1990).

[6] R. Tao and J. M. Sun, Phys. Rev. Lett. **67**, 398 (1991); Phys. Rev. A **44**, R6181 (1991).

[7] R. D. Kamien and D. R. Nelson, J. Stat. Phys. **71**, 23 (1993); Phys. Rev. A **45**, 8727 (1992).

[8] R. P. Feynman, *Statistical Mechanics* (Benjamin/Cummings, Reading, MA, 1972).

[9] D. J. Klingenberg, F. van Swol, and C. F. Zukoski, J. Chem. Phys. **91**, 7888 (1989).

[10] W. R. Toor, J. Colloid Interface Sci. **156**, 335 (1993); N. K. Jaggi, J. Stat. Phys. **64**, 1093 (1991).

[11] M. Whittle, J. Non-Newtonian Fluid Mechanics **37**, 233 (1990).

[12] D. M. Heyes and J. R. Melrose, Mol. Simul. **5**, 293 (1990).

[13] R. T. Bonnecaze and J. F. Brady, J. Chem. Phys. **96**, 2183 (1992).

[14] K. C. Hass, Phys. Rev. E **47**, 3362 (1993).

[15] For example, see, S. Chandrasekhar, Rev. Mod. Phys. **15**, 1 (1943); F. Reif, *Fundamentals of Statistical and Thermal Physics* (McGraw-Hill, New York, 1965), pp. 560–562; R. K. Pathria, *Statistical Mechanics* (Pergamon, Oxford, 1972), pp. 451–452.

[16] P. M. Adraini and A. P. Gast, Phys. Fluids **31**, 2757 (1988).

[17] For example, see, W. H. Press *et al.*, *Numerical Recipes* (Cambridge Univ. Press, Cambridge, 1987), pp. 554–560.

[18] R. Tao, Phys. Rev. E **47**, 423 (1993).

[19] K. D. Weiss and J. D. Carlson, in *Electrorheological Fluids* (Ref. [1]), p. 264.

[20] L. C. Davis, J. Appl. Phys. **72**, 1334 (1992); N. J. Félici, J. N. Foulc, and P. Atten, in Proceedings of the Fourth International Conference on ER Fluids, edited by R. Tao (World Scientific, Singapore, to be published).